Surface Reconstitution of a De Novo Synthesized Hemoprotein for Bioelectronic Applications**

Eugenii Katz, Vered Heleg-Shabtai, Itamar Willner,* Harald K. Rau, and Wolfgang Haehnel*

Electrical contacting of redox proteins and electrode surfaces is of fundamental interest in the application of redox-active biomaterials in bioelectronic devices,[1] biosensors,[2] biofuel cells,[3] and optobioelectronic systems.[4] Modification of redox enzymes with electroactive relay groups[5] or immobilization of the biocatalysts in redox-functionalized polymers[6] provide means to establish electrical communication between the redox sites in the proteins and the electrode surfaces. Recently, reconstitution of an apo-flavoenzyme on an electrode functionalized with a relay-FAD monolayer was reported to yield an aligned biocatalyst exhibiting effective electron transfer with the electrode surface.[7] This concept was further broadened to organize enzyme electrodes by cross-linking cofactor–biocatalyst affinity complexes on the electrode surface. The resulting electrically contacted enzyme electrodes were then used as biosensors.[8]

Extensive research efforts are directed to a de novo synthesis of proteins that provide wide variability in biomimetic chemistry.[9, 10] In particular, preparing synthetic proteins by antiparallel α-helix elements on a cyclic peptide is an efficient strategy for the synthesis of predetermined structures.[11] This method was successfully applied to tailor a synthetic cytochrome b analogue by the assembly of four antiparallel helices containing two heme binding sites in the hydrophobic interior.[12] The elucidation of catalytic properties and customized redox functions of these synthetic proteins remains a challenging perspective for future nanoscale bioelectronics.

Here we report on the assembly of a four-bundle synthetic protein as a monolayer on a Au electrode. We demonstrate the stepwise reconstitution of two Fe^{III}–protoporphyrin IX complexes into the synthetic protein. The resulting reconstituted protein reveals electrical contact with the electrode surface. Vectorial electron transfer proceeds in the aligned redox-active monolayer assembly, leading the synthetic hemoprotein to act as a rectifier. We also demonstrate that the synthetic hemoprotein functions as an electron transfer mediator for the native redox protein, nitrate reductase, and that the bioelectrocatalyzed reduction of nitrate is activated.

[*] Prof. I. Willner, Dr. E. Katz, V. Heleg-Shabtai
Institute of Chemistry
The Hebrew University of Jerusalem
Givat Ram, Jerusalem 91904 (Israel)
Fax: (+972) 2-6527715
E-mail: willnea@vms.huji.ac.il
Prof. W. Haehnel, H. K. Rau
Institute für Biologie II/Biochemie der Universität Freiburg
Schänzlestrasse 1, D-79104 Freiburg (Germany)
E-mail: haehnel@uni-freiburg.de

[**] This project was supported by the BMBF/Beo22 and by the Volkswagen Stiftung.

The structure of the synthetic de novo synthesized protein is shown in Scheme 1. The protein consists of 128 amino acids and has a mass of 14728 Da. It was prepared[12] from unprotected peptides (previously purified by HPLC) by the reaction of *N*ε-(bromoacetyl)lysine residues (of helix B) and

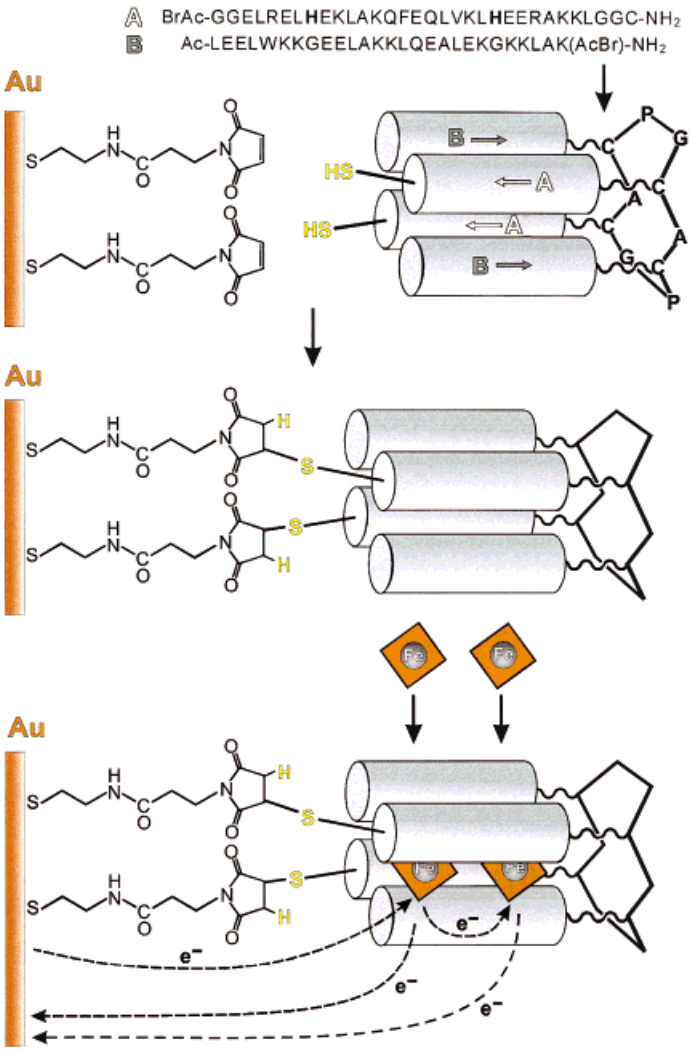

Scheme 1. Stepwise assembly of the monolayer of Fe^{III}-protoporphyrin reconstituted de novo synthetic protein on a Au electrode.

bromoacetyl glycine residues (of helix A) which were coupled to cysteine SH groups of the template. Flexible Gly-Gly-Cys units are part of the two helices A and provide a means for the covalent attachment of the de novo protein on an electrode surface. There are two histidine residues in each of the "A" helix bundles. The histidine units are positioned to allow axial ligation to the Fe^{III}–heme sites.

Scheme 1 also depicts the assembly of the synthetic protein as a monolayer on the Au surface. Coupling of a heterobifunctional reagent, *N*-succinimidyl-3-maleimidopropionate, to a cysteamine monolayer associated with a Au electrode was followed by covalent linkage of the terminal maleimide functionalities to the thiol groups of the protein.[13] The resulting monolayer was allowed to interact with Fe^{III}–protoporphyrin IX. The inset of Figure 1 A shows the cyclic

  1433-7851/98/3723-3253 $ 17.50+.50/0

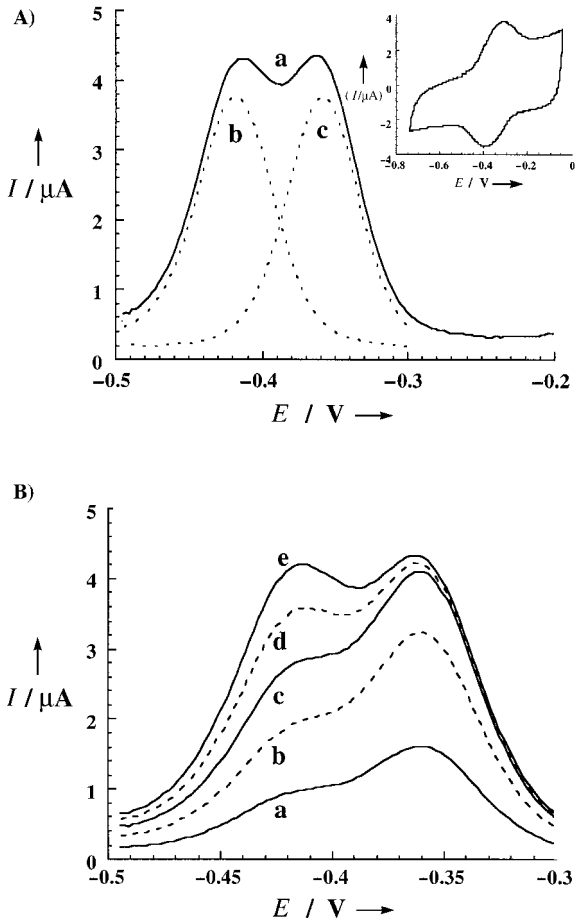

Figure 1. A) Differential pulse voltammogram (a) and deconvoluted voltammograms (b, c) of the monolayer of Fe^{III}–protoporphyrin IX reconstituted synthetic protein on the surface of the Au electrode. Inset: Cyclic voltammogram of the Fe^{III}-protoporphyrin reconstituted synthetic protein (scan rate 200 mV s^{-1}). B) Differential pulse voltammograms (scan rate 20 mV s^{-1}, pulse height 2 mV) of the synthetic proteins after reconstitution with Fe^{III}–protoporphyrin IX for 20 (a), 40 (b), 60 (c), 80 (d), and 100 min (e). Reconsitution was performed in DMSO with a Fe^{III}–protoporphyrin IX concentration of 1×10^{-4} M. The experiments were performed in 0.1 M phosphate buffer (pH 7.0) at 25 °C; electrode geometrical area 0.2 cm^2, roughness factor 1.3. I = current, E = potential vs. SCE.

voltammogram of the Fe^{III}–protoporphyrin IX reconstituted monolayer. A single redox wave is observed. Differential pulse voltammetry reveals that the electrical response of the heme consists of two overlapping redox waves (Figure 1 A). These waves were deconvoluted to two separate electrochemical processes: The reduction potential of one heme center is -0.423 V [versus the saturated calomel electrode (SCE)], and the reduction potential of the second heme center is shifted by about $+66$ mV to -0.357 V. These values are in agreement with those found for the soluble variant of the protein.

Coulometric analysis of the redox waves of the two heme sites reveals that the two Fe^{III}–protoporphyrin IX units occupy the protein bundle in a 1:1 ratio, and that the surface coverage of the heme-reconstituted synthetic protein is 2.5×10^{-11} mol cm^{-2}. Similar cyclic and differential pulse voltammograms were obtained by the coupling of a synthetic hemoprotein reconstituted with Fe^{III}-protoporphyrin IX in solution to the electrode. Assuming that the diameter of the base of the four-helix bundle is about 25 Å, the theoretical surface concentration of densely packed cylindrical four-helix bundles is around 2.7×10^{-11} mol cm^{-2}. Thus, we conclude that the resulting coverage by the four-helix bundles corresponds to an almost densely packed monolayer configuration.

Figure 1 B shows the differential pulse voltammetry waves of the monolayer upon interaction with Fe^{III}–protoporphyrin IX for different time intervals. It is evident that the heme site exhibiting the slightly more negative redox potential reconstitutes more slowly into the synthetic protein. The results indicate that the individual redox potentials of the heme sites can be tuned by the protein environment at the binding site.

Figure 2 A depicts the chronoamperometric response of the heme-reconstituted protein monolayer. For the two heme sites, positioned at different distances, a biexponential decay of the current is expected, where the fast electron transfer should occur to the heme positioned close to the electrode.[14]

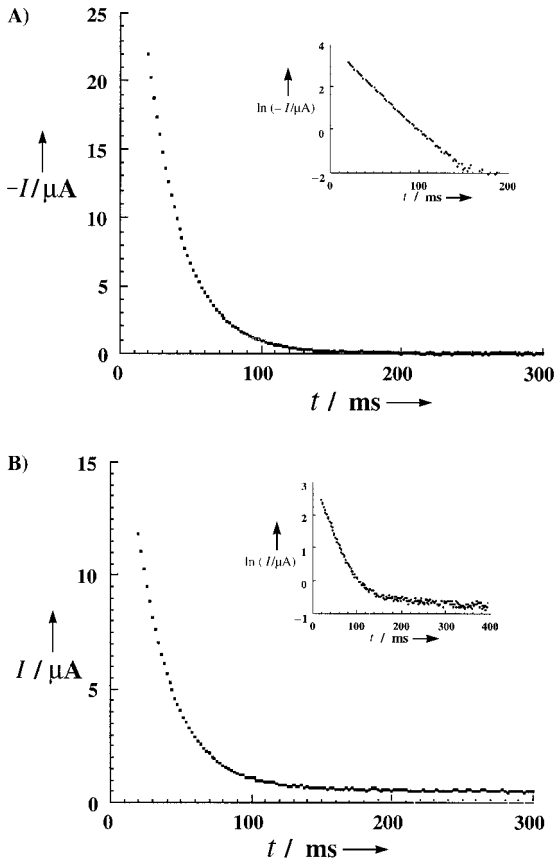

Figure 2. A) Chronoamperometric response upon reduction of the monolayer of the Fe^{III}–protoporphyrin IX reconstituted synthetic protein on the electrode (potential step from -0.2 to -0.5 V vs. SCE). Inset: semilogarithmic analysis of the decay of the current upon reduction. B) Chronoamperometric response upon oxidation of the monolayer of the Fe^{III}–protoporphyrin IX reconstituted synthetic protein on the electrode (potential step from -0.6 to -0.3 V vs. SCE). Inset: Semilogarithmic analysis of the decay of the current upon oxidation. All experiments were performed in 0.1 M phosphate buffer (pH 7.0) at 25 °C. I = current, E = potential vs. SCE.

  1433-7851/98/3723-3254 $ 17.50+.50/0

The resulting transient current, however, follows a single-exponent electron transfer rate (inset of Figure 2A). This is attributed to a vectorial electron transfer in the bifunctional Fe^{III}–protoporphyrin IX array (Scheme 1). The rate constant for single electron transfer corresponds to the fast electron transfer to the heme site close to the electrode. Secondary, fast electron transfer to the second heme center that is mediated by the heme site close to the electrode competes with long-range direct electron transfer from the electrode to the second heme site. As a result, the rate of reduction of the bifunctional assembly is controlled by the rate of electron transfer to the heme center close to the electrode. These results imply that the heme center exhibiting the more negative potential is positioned close to the electrode, which results in the electron transfer cascade. Thus, the fact that the Fe^{III}–protoporphyrin unit exhibiting the more negative potential reconstitutes more slowly into the protein can be explained by the hindrance involved in the binding of the heme positioned close to the electrode surface. This conclusion, with regard to the vectorial electron transfer cascade in the synthetic hemoprotein, is supported by following the chronoamperometric response to the oxidation of the reduced assembly (Figure 2B). The oxidation involves a biexponential decay of the current with two components, one for a fast electron transfer ($k = 40\ s^{-1}$) and one for a slow electron transfer ($k = 1\ s^{-1}$; inset of the Figure 2B). The rate of the fast electron transfer is identical to that observed in the reduction, and hence corresponds to the oxidation of the Fe^{II}–heme site close to the electrode surface. The rate of the slow electron transfer is attributed to the oxidation of the remote Fe^{II} center. The slow electron transfer is detected, since the heme center close to the electrode cannot mediate the oxidation due to its more negative redox potential. Thus, the bifunctional heme–de novo protein assembly represents elements of a bioelectronic rectifier. Vectorial electron transfer proceeds effectively in the system due to appropriate ordering of the reduction potentials of the heme centers. The back electron transfer to the electrode is retarded since the primary heme site, close to the electrode, acts as a barrier for the oxidation process.

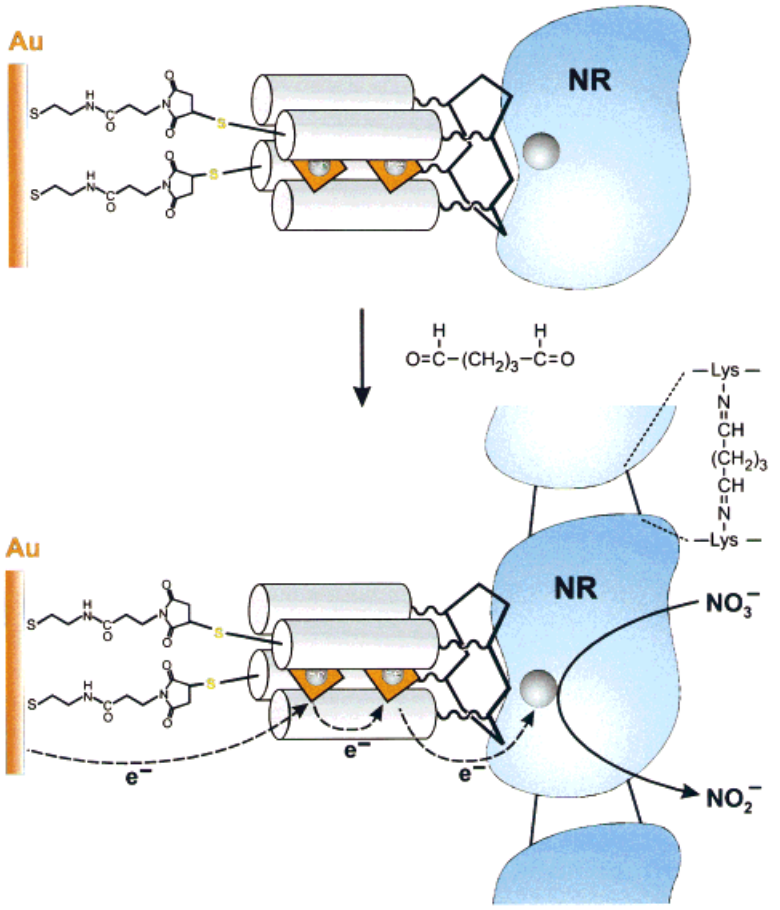

Scheme 2. Assembly of the integrated layered electrode composed of nitrate reductase (NR) and the Fe^{III}–protoporphyrin IX reconstituted synthetic protein.

The electrically contacted de novo hemoprotein monolayer associated with the electrode activates electron transfer to native redox proteins, and stimulates bioelectrocatalyzed transformations. Interaction of the synthetic bifunctional hemoprotein monolayer on the electrode with the native cytochrome-dependent nitrate reductase (NR; E.C. 1.9.6.1 from *E. coli*) results in the formation of an affinity complex (Scheme 2). Evidence for this was provided by microgravimetric quartz crystal microbalance studies. The association of nitrate reductase to the cyclic scaffold of the protein is supported by the fact that the de novo protein is in a densely packed configuration. The resulting affinity complex was cross-linked with glutaric dialdehyde to yield a stable and integrated bioelectrocatalytically active electrode.

Figure 3 shows the cyclic voltammogram of the resulting integrated enzyme electrode. The electrocatalytic cathodic current observed in the presence of added nitrate (NO_3^-) indicated the bioelectrocatalyzed reduction of NO_3^- at the potential characteristic of the synthetic hemoprotein. Control experiments revealed that no bioelectrocatalyzed reduction of NO_3^- occurs in the absence of NR, or upon direct coupling of the native biocatalyst (NR) to the base monolayer of maleimide on the electrode. Thus, the synthetic hemoprotein associated with the electrode stimulates electron transfer to NR, and the mediated electron transfer activates the bioelectrocatalyzed reduction of NO_3^-. The amperometric response of the integrated bioelectrocatalytic electrode is controlled by the concentration of nitrate (inset of Figure 3).

In conclusion, we have addressed the assembly of a bifunctional Fe^{III}–protoporphyrin de novo protein monolayer on a Au electrode, and demonstrated the electrical

  1433-7851/98/3723-3255 $ 17.50+.50/0

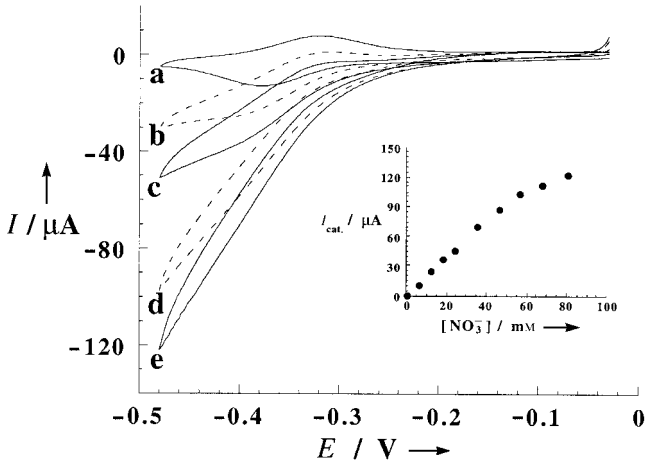

Figure 3. Cyclic voltammograms of the integrated layered electrode composed of cross-linked nitrate reductase and the Fe^{III}–protoporphyrin IX reconstituted de novo protein at NO_3^- concentrations of 0 (a), 12 (b), 24 (c), 46 (d), and 68 mM (e) (scan rate 5 mV s^{-1}). Inset: Calibration curve for the amperometric responses (at −480 mV vs. SCE) of the electrode at different NO_3^- concentrations. All experiments were performed in 0.1 M phosphate buffer (pH 7.0) at 25 °C; electrode geometrical area 0.2 cm^2, roughness factor ≈20. I = current, E = potential vs. SCE.

contacting of the synthetic redox protein with the conductive support. We presented the organization of the synthetic redox protein by the reconstitution of Fe^{III}–protoporphyrin IX into the protein, and discussed the use of this functionalized electrode for bioelectronic applications. Specifically, we demonstrated the activity of the electrically contacted bifunctional synthetic heme as a bioelectronic rectifier and as a base interface to organize integrated enzyme electrodes for biosensor applications. The potential perspectives of such reconstituted, electrically contacted de novo proteins seem to be very broad as the function of the de novo protein can be tuned and tailored within the synthetic protocol.

Received: June 8, 1998 [Z11957IE]
German version: *Angew. Chem.* **1998**, *110*, 3443–3447

Keywords: biosensors · electron transfer · enzyme catalysis · monolayers · proteins

[1] W. Göpel, *Biosens. Bioelectron.* **1995**, *10*, 35–59.
[2] a) P. N. Bartlett in *Biosensor Technology, Fundamentals and Applications* (Eds.: R. P. Buck, W. E. Hatfield, M. Umaña, E. F. Bowden), Marcel Dekker, New York, **1990**, chap. 7, pp. 95–115; b) A. Heller, *J. Phys. Chem.* **1992,** *96*, 3579–3587; c) I. Willner, E. Katz, B. Willner, *Electroanalysis* **1997,** *9*, 965–977; d) E. Katz, V. Heleg-Shabtai, B. Willner, I. Willner, A. F. Bückmann, *Bioelectrochem. Bioenerg.* **1997,** *42*, 95–104.
[3] a) I. Willner, G. Arad, E. Katz, *Bioelectrochem. Bioenerg.* **1998**, *44*, 209–214; b) I. Willner, E. Katz, F. Patolsky, A. F. Bückmann, *J. Chem. Soc. Perkin Trans. 2* **1998**, 1817–1822.
[4] a) I. Willner, *Acc. Chem. Res.* **1997**, *30*, 347–356; b) I. Willner, B. Willner, *Bioelectrochem. Bioenerg.* **1997**, *42*, 43–57; c) I. Willner, S. Rubin, *Angew. Chem.* **1996**, *108*, 419–439; *Angew. Chem. Int. Ed. Engl.* **1996**, *35*, 367–385; d) I. Willner, E. Katz, B. Willner, R. Blonder, V. Heleg-Shabtai, A. F. Bückmann, *Biosens. Bioelectron.* **1997**, *12*, 337–356.
[5] a) Y. Degani, A. Heller, *J. Am. Chem. Soc.* **1988**, *110*, 2615–2620; b) W. Schuhmann, *Biosens. Bioelectron.* **1995**, *10*, 181–193; c) I. Willner, N. Lapidot, A. Riklin, R. Kasher, E. Zahavy, E. Katz, *J. Am. Chem. Soc.* **1994**, *116*, 1428–1441.
[6] a) A. Heller, *Acc. Chem. Res.* **1990**, *23*, 128–134; b) I. Willner, E. Katz, N. Lapidot, P. Bäuerle, *Bioelectrochem. Bioenerg.* **1992**, *29*, 29–45.
[7] I. Willner, V. Heleg-Shabtai, R. Blonder, E. Katz, G. Tao, A. F. Bückmann, A. Heller, *J. Am. Chem. Soc.* **1996**, *118*, 10321–10322.
[8] a) A. Bardea, E. Katz, A. F. Bückmann, I. Willner, *J. Am. Chem. Soc.* **1997**, *119*, 9114–9119; b) V. Heleg-Shabtai, E. Katz, S. Levi, I. Willner, *J. Chem. Soc. Perkin Trans. 2* **1997**, 2645–2651; c) V. Heleg-Shabtai, E. Katz, I. Willner, *J. Am. Chem. Soc.* **1997**, *119*, 8121–8122.
[9] a) W. F. DeGrado, Z. R. Wassermann, J. D. Lear, *Science* **1989**, *243*, 622–628; b) M. Mutter, S. Vuilleumier, *Angew. Chem.* **1989**, *101*, 551–571; *Angew. Chem. Int. Ed. Engl.* **1989**, *28*, 535–554; c) J. W. Bryson, S. F. Betz, H. S. Lu, D. J. Suich, H. X. Zhou, K. T. O'Neil, W. F. DeGrado, *Science* **1995**, *270*, 935–941; d) R. B. Hill, W. F. DeGrado, *J. Am. Chem. Soc.* **1998**, *120*, 1138–1145; e) B. R. Gibney, S. E. Mulholland, F. Rabanal, P. L. Dutton, *Proc. Natl. Acad. Sci. USA* **1996**, *93*, 15041–15046.
[10] a) C. T. Choma, J. D. Lear, M. J. Nelson, P. L. Dutton, D. E. Robertson, W. F. DeGrado, *J. Am. Chem. Soc.* **1994**, *116*, 856–865; b) D. E. Robertson, R. S. Farid, C. C. Moser, J. L. Urbauer, S. E. Mulholland, R. Pidikiti, J. D. Lear, A. J. Wand, W. F. DeGrado, P. L. Dutton, *Nature* **1994,** *368*, 425–432; c) F. Rabanal, W. F. DeGrado, P. L. Dutton, *J. Am. Chem. Soc.* **1996**, *118*, 473–474; d) F. Arai, K. Kobata, H. Mihara, T. Fujimoto, N. Nishino, *Bull. Chem. Soc. Jpn.* **1995**, *68*, 1989–1998.
[11] M. Mutter, E. Altmann, K.-H. Altmann, R. Hersperger, P. Koziej, K. Nebel, G. Tuchscherer, S. Vuilleumier, H. U. Gremlich, K. Müller, *Helv. Chim. Acta* **1988**, *71*, 835–847.
[12] H. K. Rau, W. Haehnel, *J. Am. Chem. Soc.* **1998**, *120*, 468–476.
[13] From the surface coverage of the base monolayer of maleimide (4.8×10^{-11} mol cm^{-2}), we estimate an average intermolecular distance of 18 Å between the residues. This value is almost identical to the distance separating the two helices carrying the cysteine sites, and hence a bifunctional linkage of the de novo protein is assumed.
[14] E. Katz, I. Willner, *Langmuir* **1997**, *13*, 3364–3373.

  1433-7851/98/3723-3256 $ 17.50+.50/0